Monitoring the waiting time sequence of single Ras GTPase activation events using liposome functionalized zero-mode waveguides

Supporting Information

Sune M. Christensen, Meredith G. Triplet, Christopher Rhodes, Jeffrey S. Iwig, Hsiung-Lin Tu, Dimitrios Stamou, Jay T. Groves[*]

*Correspondence: jtgroves@lbl.gov

METHODS

Fabrication and functionalization of ZMWs for liposome immobilization

A #1 glass slide (Fisher Scientific) was pre-cleaned and plasma etched for 5 minutes. Thermal deposition of aluminum (99.9% purity Al pellet, Kurt J. Lesker Company) was achieved using an NRC evaporator and single-use tungsten baskets (Mathis Company, Long Beach, CA). During deposition, pressure was less than $5x10^{-6}$ Torr. Current was monitored manually to maintain a deposition rate of 0.1–0.2 nm/s. The total thickness was measured using a crystal monitor. Deposition was stopped by shutter when 75–100 nm total thickness was achieved.

Zero-Mode Waveguides (ZMWs) were etched into the aluminum surface with a FEI Quanta FIB. This instrument has a dual-beam SEM that was used to periodically assess quality of focus during fabrication. Alignment marks were etched on each substrate to optimize beam focus and facilitate microscope localization of the area of interest. A mask with a 12x12 grid of 100 nm diameter circles and 2.5 μm pitch was used to pattern each substrate. Grids were arranged in groups of four for maximum imaging throughput (576 per field of view). To achieve a range of waveguide sizes, etching power and time were in the ranges of 50 pa-0.25 nA and 100–750 ms, respectively.

Prior to experimentation, the ZMW substrate was plasma etched for 30 s, mounted in a pre-cleaned teflon microscope chamber (custom made) and incubated for 30 min. with a 1:5 mixture of PLL(20)-g[3.5]-PEG2 : PLL(20)-g[3.5]-PEG2/PEG-(3.4)-Biotin(20%) (SuSoS, Dübendorf, Switzerland). The substrate was then washed copiously in buffer, incubated for 10 min. with 0.05 g/l Neutravidin (Sigma-Aldrich, St. Luis, MO) followed by another washing cycle.

Protein purification and labeling

SOS: SOS^{Cat} (residues 566-1049 with following mutations: C838A, C635A, C980S, E718C) and SOS-DPC (residues 198-1049) of human SOS1 were expressed in *E. Coli* and purified as previously described[1]. Labeling of SOS constructs with Atto647N-maleimide was carried out by reacting 1:10 molar ratio of purified protein with the dye for 2 hours at 23°C. Unreacted fluorophores were removed using PD-10 columns (GE Healthcare). Labeling efficiency was assessed by UV/Vis spectroscopy (NanoDrop 2000, Thermo Scientific) yielding; 90% for SOScat cyslite and 119% for DPC. The labeling efficiency larger than 100% for DPC is explained by the DPC construct harboring multiple cysteines.

Ras: $H\text{-}Ras^{C118S,C181}$ (construct comprising residues 1-181 with a single cysteine at position C181 used for coupling to the liposome bilayer via MCC was expressed in *E. Coli* and purified as previously described[1].

Optical microscopy

Imaging was performed on an inverted microscope (Nikon Eclipse Ti (Ti HUBC/A), Technical Instruments, Burlingame, CA) equipped with a Nikon Apo TIRF 100x/1.49 oil objective. The microscope had a custom-built laser launch with 488 nm and 633 nm lasers (both from the OBIS product line, Coherent Inc. Santa Clara, CA) controlled via a laser control module (OBIS scientific remote). The 488 nm and 633 nm lasers were reflected to the specimen via dichroic mirrors and emission was collected in EPI mode. Emission signal was filtered using, respectively, ET525/50M and ET600/50 filters (Chroma, Bellows Falls, VT). Images were collected on an EM-CCD (iXon ultra 897, Andor Inc., South Windsor,

CT) and the microscope was operated using micro-manager[2]. Bright field images to locate the position of ZMWs were acquired with a Nikon Intensilight C-HGFIE lamp.

Liposome preparation

All lipids were purchased from Avanti Polar Lipids, Alabaster, AL except BODIPY 500/510 C12-HPCm, which was from Life Technologies, Carlsbad, CA. Lipids were mixed in chloroform in a round-bottomed flask. The lipid composition was 88 mol% Egg-PC: 5% MCC-DOPE:5% DOPS:1% 18:1 Biotinyl Cap PE: 1% BODIPY 500/510 C12-HPC (for SOS^{cat} measurements) and 91mol% DOPC: 5.5% MCC-DOPE:1% DOPS: 1% 18:1 Biotinyl Cap PE: 1% BODIPY 500/510 C12-HPC: 0.5% PiP_2 (in experiments with SOS^{DPC}). Chloroform was removed by 30 min. spinning on a rotary evaporator at 40 °C followed by at least 10 min. under nitrogen flow. Liposomes were formed by rehydrating the lipids in 20 mM HEPES [pH 7.0], 150 mM NaCl, 10 mM beta-mercaptoethanol. Liposomes were extruded in 3 consecutive runs using the LiposoFast mini-extruder (AVESTIN Inc., Ottawa, ON, Canada) equipped with 30 nm pore size filters (product number 800307, GE Healthcare). 365 µl vesicle suspension at 5 g/l lipid concentration was mixed with 50 µl Ras181 at 6 g/l. Coupling of the C-terminal cysteine of the Ras construct to the MCC headgroups on the liposomes was carried out at room temperature for 2.5 h. The resulting proteoliposome suspension was snap frozen using liquid nitrogen and stored at -80 °C.

Ras activation assay

All dilutions, washes and nucleotide exchange assays were done in 40 mM HEPES [pH 7.4], 5 mM $MgCl_2$, 100 mM NaCl, 1 mM TCEP. ZMW positions were located in bright field imaging mode. 10 μM EDA-ATTO488-GTP (Jena Bioscience, Gmbh) was added to the sample to check the signal in absence of nucleotide exchange activity and time-series were recorded at the different grid positions. The fluorescent nucleotide was then washed out of the chamber. Ras loaded liposomes at 5 g/l (see above) were reacted for 5 min. with 5 mM BME to quench any remaining reactivity of the MCC lipid head groups. Liposomes were then incubated with ≈300 nM SOS^{DPC}-ATTO647N or 100 nM SOS^{cat}-ATTO647N for 10 min. at room temperature and then stored at ice until injection on sample. In the absence of nucleotide, SOS gets stably recruited to the vesicles via allosteric Ras binding and locked with nucleotide-free Ras bound at the active site[3,4]. 10 μl of the SOS reacted liposomes were injected into a volume of 500 μl buffer in the ZMW mounted microscope chamber. Efficient loading of the ZMWs typically took on the order of 30 min. after which unbound vesicles and SOS were removed by washing.

A series of bright field images of the grids and corresponding EPI images were acquired to locate the liposome and SOS positions (from, respectively, BODIPY and ATTO647N fluorescence). The SOS label was then bleached by continuous illumination with high laser power (≈75 mW laser power incident on the objective) followed by bleaching of the liposome label. 10 μM EDA-ATTO488-GTP was added to the chamber to initiate the nucleotide exchange reaction and time-series were acquired at the different grids.

Fitting of single turnover traces

Data analysis was accomplished with a software suite written in Igor Pro (Wavemetrics, Lake Oswego, OR). Activity traces from single ZMWs were extracted from the time-series by integrating the intensity inside a region of interests (ROI). Prior to analysis traces were filtered to *(i)* remove baseline drift by

subtracting from the trace a running average of the trace itself calculated using the "boxcar" smoothing algorithm in Igor Pro, with a box width of 1000 points (the width was chosen as to avoid distorting the step features in the traces) and *(ii)* reduce random noise by subtracting a high pass filtered version of the trace from itself (conducted using the FilterFIR command in Igor Pro with the following flags /DIM=0/HI={0.2,0.3,101}).

Levels in the resulting traces were identified using the Bayesian change point detection algorithm developed by Ensing and Pande for Gaussian distributed data[5]. A Bayes factor of 3 was employed for level detection. The cumulative distribution of the identified intensity levels were then fitted with a double Gaussian and based on the fit a threshold was defined to categorize levels as belonging to either on or off states (see main text for definitions). The threshold was initially set to $I_h-(I_h-I_l)/4$, where I_h indicates the average of the higher intensity level and I_l the intensity of the lower intensity level. The threshold was then refined such that only a few events were detected in the control region of the traces. The change point algorithm for Gaussian distributed data is incapable of detecting levels with fewer than 4 data points and therefore an additional refinement of level identification was implemented. This was achieved by searching the assigned baseline regions for clusters of intensity values (defined as two or more consecutive points) that exceeded the local baseline with more than ¾ x $\mathbf{\Delta I}$, where $\mathbf{\Delta I} = I_h-I_l$). Identified clusters were now tested for significance using the change point algorithm of Ensing and Pande derived for binomially distributed data[5]. In this case, for each baseline region a putative change point candidate was tested by artificially moving the given cluster of data to the end of that baseline region and testing for the presence of a change point at this location. A Bayes factor of 10^6 was employed as a criteria for acceptance. Finally, dwell times and waiting times were extracted based on the identified intensity levels.

Simulations of the excitation field inside a ZMW

Finite-element simulations using COMSOL Multiphysics' RF Module were used to model the excitation field inside a ZMW containing a liposome. The Electromagnetic Waves platform was used in 3D mode to model the excitation field. A free tetrahedral mesh was used with "Extra Fine" resolution and a refinement applied to the aluminum layer. Although only one waveguide was used for the bulk of the studies, a study was done to demonstrate that the spacing between waveguides is sufficient to isolate the excitation effects. A perfectly matched layer (PML) was incorporated in the borosilicate glass component to cancel any reflection artifacts from the simulation boundaries. The waveguide was simulated in a 100 nm layer of aluminum with refractive index (RI) as 0.77 and 5.9 for the real and imaginary part, respectively, as interpolated from literature tables[6]. A 488 nm wavelength of excitation was used from the bottom of the glass module, arriving perpendicular to the plane of the aluminum thin film.

The waveguide was modeled with a width of 100 nm and with a 10 nm over-etch into the glass, with the vesicle of 50 nm diameter centered at 10 nm up from the surface. Field simulations were conducted to demonstrate that over-etching reduced the effects of increased intensity at the bottom corners of the waveguide, and that minimal (but noticeable) effects were caused by altering the vesicle's location relative to the waveguide in the x,y, and z directions, and that more of the vesicle was more highly excited for wider waveguides. The vesicle was simulated as two hollow shells with distinct RI values, with the outer layer mimicking Ras (RI 1.6 with imaginary component 10^{-9} [7] with 5 nm thickness) and the inner layer mimicking the lipid component as modeled by octane (RI 1.53 with imaginary component 10^{-9} [8] with 3.87 nm thickness[9], with the central region having the same values as the water-based buffer. Studies with varied RI demonstrated minimal sensitivity to small changes in the lipid or protein values, so these

rough approximations were deemed acceptable. A diagonal cross-section of the 3D model was used to visualize the excitation dynamics within the waveguide, and a map was also formed of the excitation intensity at the outer surface of the vesicle.

Estimating the effective excitation flux impinging on fluorophores diffusing at the membrane of a ZMW immobilized liposome

Consider a liposome tethered at the center of a zero-mode waveguide (**Fig. 1c**). From finite element simulations we have obtained a list of excitation field intensities at a set of discrete points on the liposome surface $I(x_i,y_i,z_i)$. In the experiments, we are integrating over a time bin of approximately 20 ms when imaging the fluorescence emission of dye molecules on the camera. Because dye molecules are free to diffuse at the liposome membrane they will experience a varying excitation field in the course of camera exposure. To estimate the effective excitation flux I_{Eff} experienced by a fluorophore started at height z with respect to the ZMW floor and diffusing in the course of a camera exposure we replaced each $I(x_i,y_i,z_i)$ with a weighted average over all other locations on the liposome surface as follows:

$$I_{Eff}(x,y,z) = S(x,y,z)\sum_i \frac{P(x,y,z,x_i,y_i,z_i)I(x_i,y_i,z_i)}{\rho(z_i)} \quad , \quad S = \left(\sum_i \frac{P(x,y,z,x_i,y_i,z_i)}{\rho(z_i)}\right)^{-1} \qquad \text{[eq. 1]}$$

Here $\varrho(z_i)$ denotes the density of discrete samples on the liposome surface at a given height from the ZMW surface (as defined by the simulation, due to symmetry we only consider the z component). S is a scaling factor that for a given point (x,y,z) was adjusted to comply with the normalization criterion at the right side of eq. 1. The sum runs over all discrete samples (x_i,y_i,z_i) of the excitation field. The sampling density $\varrho(z_i)$ was estimated by fitting the simulated data with an exponential function yielding the (approximated) relation:

$$\rho(z_i)[\mathrm{nm}^{-2}] = 0.248 + 7.922exp\left(-\frac{z-0.00125}{0.00121}\right) \qquad \text{[eq. 2]}$$

The weights $P(x,y,z,x_i,y_i,z_i)$ were calculated as the time-integrated probability density of finding a particle undergoing Brownian motion at a certain auxiliary point located a distance r away on the sphere surface (where r denotes the great circle distance between the point (x, y, z) and (x_i, y_i, z_i)):

$$P(r(x_i,y_i,z_i),t,D) \;=\; \int_{t_0}^{t_1} \frac{1}{4\pi Dt} exp\left(-\frac{r^2}{4Dt}\right) dt \qquad \text{[eq. 3]}$$

t_0 was taken as 1 μs (to circumvent the discontinuity at t=0) and t_1=20 ms, the exposure time on the camera. The great circle distance, r, is a function of the point in consideration (given by the vector r_2 pointing from the center of the sphere, $C(x_c, y_c, z_c)$, to the given point on the liposome surface) and the auxiliary point (given by the vector r_2)):

$$
\begin{aligned}
r_1 &= \langle x - x_c, y - y_c, z - z_c \rangle \\
r_2 &= \langle x_i - x_c, y_i - y_c, z_i - z_c \rangle \\
r(x, y, z, x_i, y_i, z_i) &= R \quad cos^{-1} \left(\frac{(x - x_c)(x_i - x_c) + (y - y_c)(y_i - y_c) + (z - z_c)(z_i - z_c)}{R^2} \right)
\end{aligned}
$$

[eq. 4]

Where *R* denotes the radius of the sphere. Combining equation 1-4 above yields the effective excitation field shown in Supporting Information Figure 3 (t=20 ms). The solution was evaluated numerically.

The provided estimation is intended as a qualitative gauge for the order of magnitude of the diffusion effect. In this regard, it is important to note that we observe clear plateaus from single molecule signals in the traces, which is only expected if diffusion effectively cancels out the heterogeneity in the excitation field.

Methods Section References

1. Gureasko, J.; Galush, W. J.; Boykevisch, S.; Sondermann, H.; Bar-Sagi, D.; Groves, J. T.; Kuriyan, J. *Nat. Struct. Mol. Biol.* **2008,** 15, (5), 452-61.

2. Edelstein A.; Amodaj N.; Hoover K.; Vale R., Stuurman N. *Curr. Prot. Mol. Biol.* (John Wiley & Sons, New York) **2001**.

3. Bos, J.L.; Rehmann, H.; and Wittinghofer, A. *Cell* **2007**, 129, (*130)*, 385-385.

4. Iversen, L.; Tu, H. L.; Lin, W. C.; Christensen, S. M.; Abel, S. M.; Iwig, J.; Wu, H. J.; Gureasko, J.; Rhodes, C.; Petit, R. S.; Hansen, S. D.; Thill, P.; Yu, C. H.; Stamou, D.; Chakraborty, A. K.; Kuriyan, J.; Groves, J. T. *Science* **2014**, 345, (6192), 50-4.

5. Ensing, D.L. and Pande, V. S. *J. Phys. Chem. B* **2010**, 114, 280-292.

6. Palik, E.D. *Handbook of Optical Constants of Solids*. (Academic, Amsterdam) **1998**.

7. Voros J. *Biophys J*., **2004**, 87, 553–561.

8. Costner, EA; Long, BK; Navar, C; Jockusch, S; Lei, X; Zimmerman,P; Campion, A; Turro, NJ Willson, CG *J. Phys. Chem.* A **2009**, 113, 9337-9347.

9. King, G.I., White, S.H. *Biophys. J.* **1986**, 49, 1047–1054.

SUPPLEMENTARY FIGURES

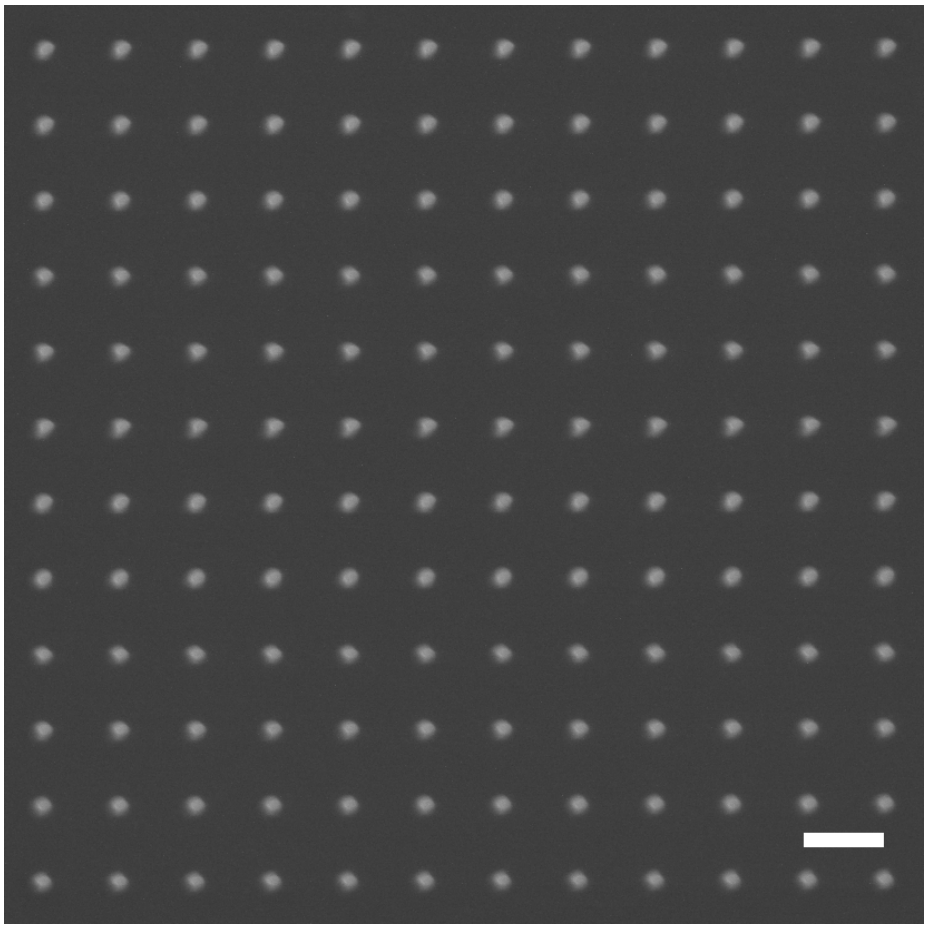

Supplementary Figure 1. SEM image of ZMW grid. Bar: 2.5 μm.

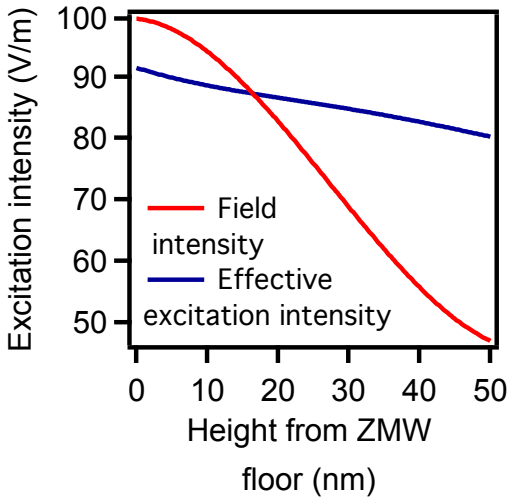

Supplementary Figure 2. Brownian diffusion balances the effect of a heterogeneous excitation field over the liposome membrane. Red trace shows the excitation field at the liposome membrane at a given height from the ZMW floor. Blue trace shows the estimated effective excitation field experienced by a fluorophore diffusing at the membrane with diffusion coefficient of 1 $\mu m^2/s$ during a camera exposure of 20 ms, when started at the membrane at a given height from the ZMW floor. See the methods for details on the calculation.

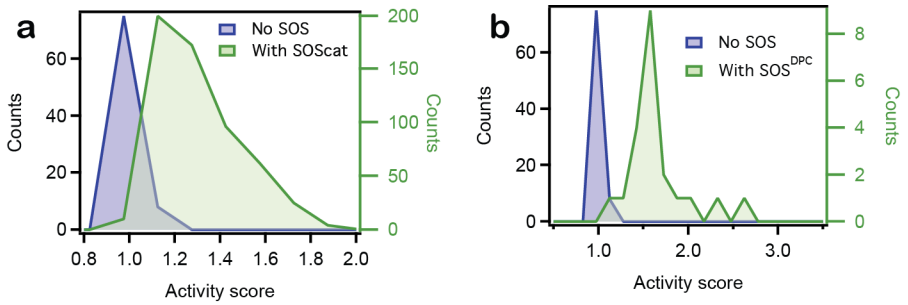

Supplementary Figure 3. Nucleotide exchange activity is specific to the presence of SOS. Histograms of activity scores recorded from arrays of ZMWs. The activity score was defined as follows: standard deviation of baseline subtracted trace (see Methods) from single ZMW in the presence of SOS divided by the standard deviation of background subtracted trace from the same ZMW in the absence of SOS. Increased fluctuation in a baseline subtracted trace upon addition of SOS corresponds to increased nucleotide exchange activity, thus resulting in an activity score above 1. In (a) liposomes were present both before and after adding SOS. In (b) the no SOS part of the traces used to obtain the activity scores was acquired without liposomes present (i.e., simply incubating labeled nucleotide on a ZMW array). Liposomes were incubated with elevated levels of SOS in order to bind SOS on all liposomes. The "With SOS" histograms in (a) and (b) comprise data from one sample each. The blue shaded "No SOS" reference histogram is the same for the two panels and was obtained by comparing traces from ZMWs before and after immobilization of liposomes but without SOS (see Figure 1g). As expected, when SOS is omitted activity scores come out around 1. The total counts for each histogram: "No SOS" (N=83), "With SOScat" (N=568) and "With SOS^{DPC}" (N=21).

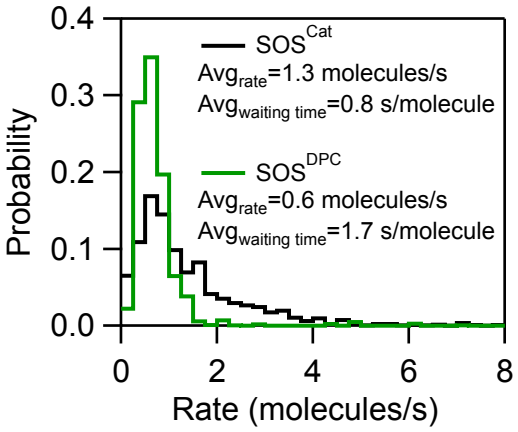

Supplementary Figure 4. Single SOS nucleotide exchange activity rate distributions for SOS^{Cat} and SOS^{DPC} recorded on supported lipid bilayers. Histogram of single SOS activity states for SOS^{Cat} and SOS^{DPC} obtained using micro-patterned supported lipid bilayers, as described in Iversen et al., *Science* **2014,** 345, (6192), 50-4. Average turnover rates and corresponding waiting times (calculated from the measured average rates) are indicated in the legend. The histogram for SOS^{DPC} comprise data from 4 supported lipid bilayer samples whereas the histogram for SOS^{Cat} comprise data from 5 samples.

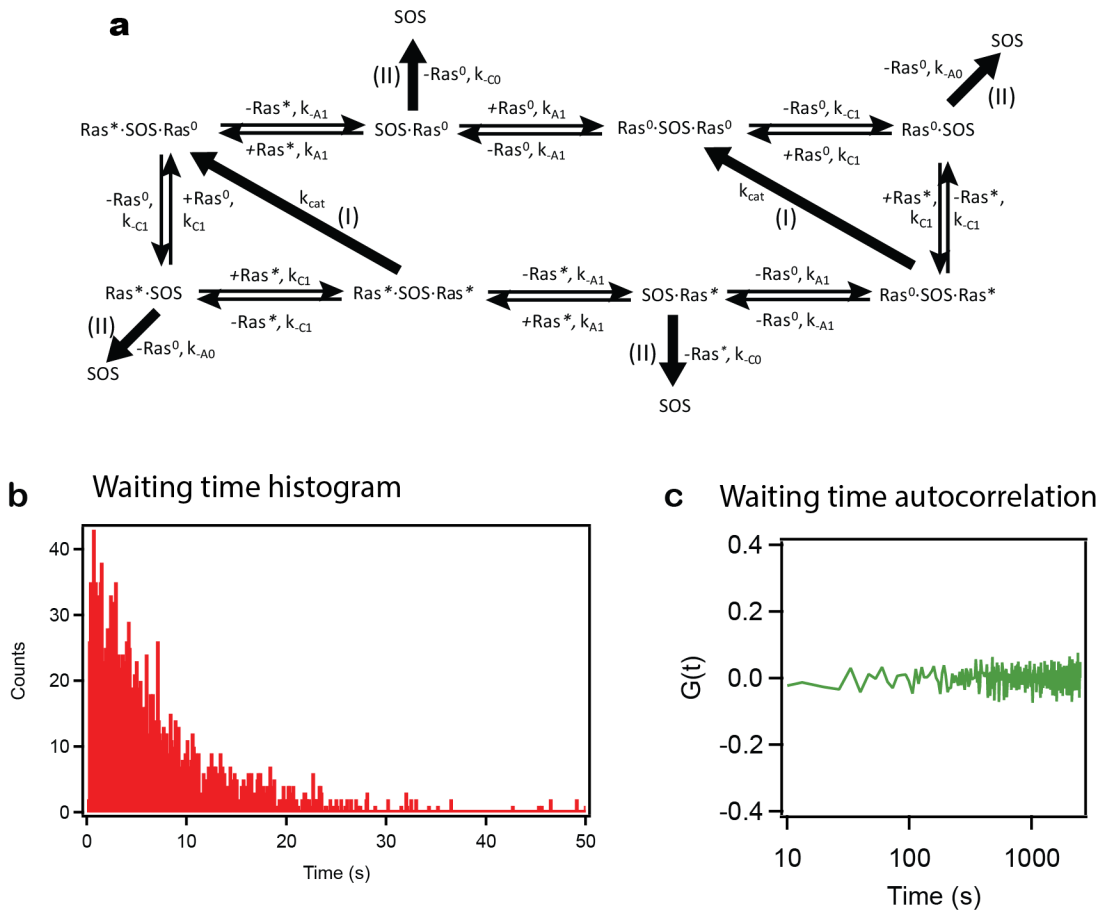

Supplementary Figure 5. Stochastic simulations of SOS catalyzed nucleotide exchange. **(a)** Reaction network for a single-state SOS molecule (i.e., working at a fixed catalytic rate) turning over Ras. Ras·SOS indicates Ras bound in the allosteric site, SOS·Ras indicates Ras bound in the catalytic site, and Ras·SOS·Ras indicates Ras in both allosteric and catalytic sites. Ras* represents a Ras loaded with fluorescent nucleotide whereas Ras0 is a Ras with non-fluorescent nucleotide. Channel (I) leads to a nucleotide exchange reaction and channel (II) describes the case where a SOS unbinds from the surface. The reaction model is adapted from Iversen et al., *Science* **2014,** 345, (6192), 50-4 **(b)** Waiting time data from a stochastic simulation based on the reaction network in a. Simulation condition: Time steps of 0.06 ms for 15,000 seconds. kcat=0.16, Ras density 4,000 molecules/μm^2. **(c)** Autocorrelation function for the waiting time list histogrammed in b. As expected for a SOS enzyme catalyzing nucleotide exchange at a fixed catalytic rate, G(t) indicates that subsequent waiting times are entirely uncorrelated. The simulation was performed using the simulation procedure reported in Iversen et al., *Science* **2014,** 345, (6192), 50-4. The simulation was repeated twice.